

## Neoclassical Energy Confinement in Stellarators

W. LOTZ, J. NÜHRENBURG, AND A. SCHLÜTER

*Max-Planck-Institut für Plasmaphysik, IPP-EURATOM Association,  
D-8046 Garching bei München, West Germany*

Received April 3, 1986

Neoclassical energy confinement times in  $l=2$  stellarators and tokamaks with and without ripple are computed by Monte Carlo simulation over wide ranges of mean free paths, ratios of plasma to gyro radius, and radial electric fields. In parameter ranges which allow computation of a local neoclassical heat conduction, this quantity is also obtained by Monte Carlo simulation and related to the energy confinement. The plateau,  $\nu^{-1}$ ,  $\nu^{1/2}$ , and  $\nu$  regimes are discussed. © 1987 Academic Press, Inc.

### 1. INTRODUCTION

In this paper, Monte Carlo methods developed previously [1–3] for calculating neoclassical heat conductivity in stellarators are generalized to the calculation of energy confinement times for stellarators. This generalization allows one to treat not only the limiting case of a large ratio  $Q_\rho$  of plasma radius  $a$  to gyro radius  $\rho$  in which a local transport coefficient can be calculated, but also cases in which the gyro radius is too large for a strictly local transport coefficient to exist. A simple criterion for the non-existence of local heat conductivity is the loss of test particles before a heat conduction coefficient can be calculated from the spatial broadening of an initially localized distribution of test particles. For mean free paths larger than the connection length, this behaviour is seen for values of  $Q_\rho$  of the order of  $10^2$ . Experimentally,  $Q_\rho$  is of the same order for thermal ions in existing stellarators (W VII A and Heliotron), in stellarators currently being built (W VII AS, ATF), and probably also in next-generation stellarators (e.g., W VII X), so that it is important to assess the effects of a finite value of  $Q_\rho$  [4]. The effect of an electric field is important for the local heat conductivity in the long mean free path (lmfp) regime since it changes the collisionless particle orbits; for the computation of energy confinement times the effects of an electric field are even more important, since, in addition, it governs the spatial profile of the test particle distribution function. Therefore, an electric field  $F$  is included in the form of an electric potential  $\phi$  which is constant on magnetic surfaces. As in earlier work, the problem of Monte Carlo simulation of the transport properties is alleviated by the assumption of a monoenergetic test particle distribution with energy  $E$ . The basic tool used is the Fowler–Rome–Lyon code [3], which, because it is formulated in magnetic coor-

dinates [5], allows an electric potential more easily than the Monte Carlo code in Cartesian coordinates [2]. Detailed tests (without electric field) have shown complete agreement between the results of these two codes if a sufficient number of Fourier coefficients representing  $|\mathbf{B}|$  in magnetic coordinates are taken into account [6].

This paper is organized as follows. Section 2 describes the Monte Carlo procedure which yields a stationary test particle distribution and an associated energy confinement time. In Section 3 results are obtained for  $l=2$  stellarators. In the appropriate regions of mean free path and value of  $Q_\rho$ , the diffusion coefficient and energy confinement time are related to each other. The so-called  $\nu$  regime (i.e., the very long mean free path regime) is investigated and the result is explained in terms of a model for the loss-cone-dominated distribution function. In Section 4 an electric field is taken into account and the collision operator is appropriately complemented. The effect of the potential on the loss rate in the plateau regime is discussed. In Section 5 results are presented for  $l=2$  stellarators, with electric fields taken into account. Results for more general stellarators are obtained without changes in the procedure, since only a different Fourier structure of  $|\mathbf{B}|$  has to be used as input for the Monte Carlo code. Some results for more general stellarators are contained in [7] and will be presented in a subsequent paper.

## 2. STATIONARY DISTRIBUTION AND ENERGY CONFINEMENT TIME

If the value of  $Q_\rho$  is sufficiently large, a local heat conduction coefficient can be calculated with the help of Boozer's Monte Carlo equivalent of the pitch angle scattering operator. The results can be presented in a normalized way [2] and are briefly repeated here for tokamaks without and with ripple and for  $l=2$  stellarators. A dimensionless mean free path  $L^*$  is used:

$$L^* = A/L_c, \quad L_c = \pi R_0/l, \quad (2.1)$$

where  $A$  is the mean free path,  $L_c$  half the connection length,  $R_0$  the major torus radius, and  $l$  the rotational transform (or twist) on the magnetic surface considered. A dimensionless transport coefficient  $D^*$  is introduced by

$$D^* = D/D_p, \quad (2.2)$$

where  $D_p$  is the plateau value

$$D_p = 0.64 \frac{\rho^2 v}{l^2 L_c} = 0.64 \frac{\rho^2 v}{l \pi R_0}, \quad (2.3)$$

$v = (2E/m)^{1/2}$  being the particle velocity and  $\rho = mv/eB_0$  the formal gyro radius, where  $B_0$  is the main magnetic field at  $R_0$ .

With these normalizations, the Pfirsch-Schlüter regime, the tokamak banana regime, and the ripple regime are given, respectively, by

$$D_{\text{PS}}^* = 1/L^*, \quad D_{\text{B}}^* \approx A^{1.5}/L^*, \quad D_{\text{R}}^* = 1.65 \delta_{\text{e}}^{1.5} L^*, \quad (2.4)$$

where  $A = R_0/r$  is the aspect ratio of the magnetic surface considered and  $\delta_{\text{e}}$  is the effective ripple.

For an  $l=2$  stellarator of  $N$  field periods, a more precise representation of ripple transport is given by

$$D_{\text{R}}^* = 2.33 A^{-2.35} i N L^* \quad (2.5)$$

for  $10 \leq A \leq 40$ ,  $0.25 \leq i \leq 1.0$ ,  $5 \leq N \leq 19$ .

An alternative affording wider applicability is to assess the neoclassical ion behaviour by computing an energy confinement time  $\tau$  (or, equivalently, a loss rate  $S = 1/\tau$ ) from an asymptotic stationary distribution which is obtained as follows. Only scattering with a uniform background plasma is considered, so that a constant value of mean free path for pitch angle scattering is assumed throughout the plasma volume. A particle carrying energy across the boundary of this volume is replaced by another particle with the same initial energy  $E$  in such a way that a particle (with index  $n_i$ ) of the remaining test distribution is doubled and from then on treated as statistically independent. The particle to be doubled is selected according to a cyclic procedure

$$n_i = (n_{i-1} + k_{\text{cyc}}) \quad \text{modulo } 64 \quad (2.6)$$

for a test distribution which comprises 64 particles. Here,  $n_{i-1}$  is the index of the particle which was doubled last. The cycle number  $k_{\text{cyc}}$  has to be relative prime to the number of particles. By this procedure a stationary solution is asymptotically obtained and corresponds to the slowest decay mode of the drift kinetic equation without source term. The decay rate of this mode corresponds to the Monte Carlo replenishment rate and is equivalent to the energy loss rate. Asymptotically in time the procedure described is equivalent to a particle source function proportional to the distribution function (see also Eq. (3.4)).

A stationary distribution obtained in this way is shown in Fig. 1. In conjunction with this distribution, the following plateau loss rate is found:

$$S_{\text{P}} = 3.6 \frac{v}{Q_{\rho}^2 i \pi R_0}. \quad (2.7)$$

Comparison of Eqs. (2.3) and (2.7) yields the well-known result [8]

$$\frac{D_{\text{P}}}{S_{\text{P}}} = \left( \frac{a}{2.4} \right)^2, \quad (2.8)$$

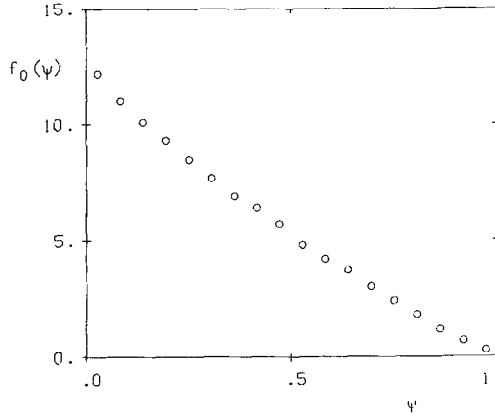


FIG. 1. Stationary distribution function  $f_0(\psi)$  in a tokamak in the plateau regime. The distribution was obtained from the asymptotic behaviour in time ( $10^5$  collision times).  $L^* = 10$ ,  $Q_\rho = 10^3$ ,  $R_0/a = 10$ ,  $\iota = 0.5$ .

which may also be considered as a validation of the Monte Carlo procedure for obtaining this loss rate. It is useful to keep the following sets of numbers in mind:

$$E(\text{deuterons}) = 10 \text{ keV}, \quad a = 1 \text{ m}, \quad R = 10 \text{ m}, \quad B = 5 \text{ T}, \quad \iota = 0.5, \quad S_P \approx 4 \text{ sec}^{-1};$$

$$E(\text{protons}) = 3 \text{ keV}, \quad a = 0.5 \text{ m}, \quad R = 5 \text{ m}, \quad B = 3 \text{ T}, \quad \iota = 0.5, \quad S_P \approx 9 \text{ sec}^{-1}.$$

In a way analogous to Eq. (2.2), normalized loss rates can be introduced by

$$S^* = S/S_P. \quad (2.9)$$

For the Pfirsch-Schlüter, banana, and, in the case of a rippled tokamak, ripple regimes, results completely analogous to Eq. (2.4) are found:

$$S_{PS}^* = 1/L^*; \quad S_B^* \approx A^{1.5}/L^*; \quad S_R^* = 1.65 \delta_e^{1.5} L^*. \quad (2.10)$$

Figure 2 shows these results.

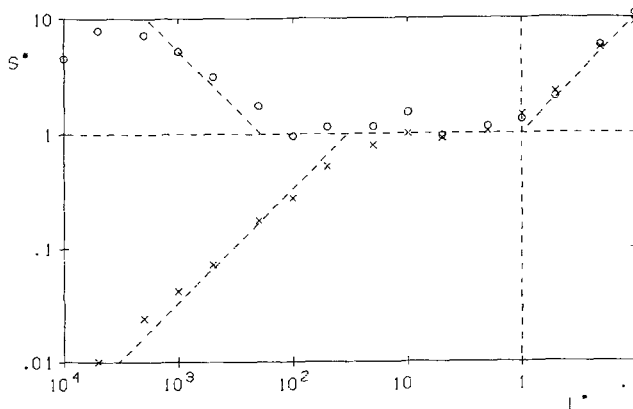


FIG. 2. Normalized loss rates in a tokamak without and with ripple.  $Q_\rho = 10^3$ ,  $R_0/a = 10$ ,  $\iota = 0.5$ ,  $\delta_e = 0.02$ .

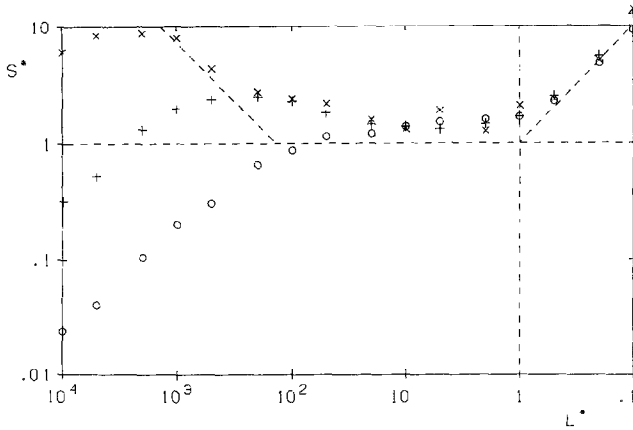


FIG. 3. Normalized loss rates in an  $l=2$  stellarator for  $Q_\rho = 50$  ( $\circ$ ), 200 ( $+$ ), and 1000 ( $\times$ ).  $R_0/a = 8.6$ ,  $N = 5$ ,  $\iota = 0.5$ ,  $\delta_e \approx 0.02$  (at aspect ratio  $A = 17$ ).

### 3. RESULTS FOR $l=2$ STELLARATORS WITHOUT ELECTRIC FIELD

Results analogous to those for rippled tokamaks are found for  $l=2$  stellarators and shown in Fig. 3. The ripple regime can be described by (compare Eq. (2.5))

$$S_R^* \approx 2.33(2A)^{-2.35} \iota NL^* = 0.46A^{-2.35} \iota NL^*. \quad (3.1)$$

The curves in Fig. 3 show the behaviour of the loss rate in the very long mean free path regime, where, for the plasma to gyro radius ratio chosen, a local transport coefficient no longer exists. In good approximation this so-called  $\nu$  regime is given by

$$S_\nu \approx \frac{\nu}{A} = \nu, \quad (3.2)$$

$\nu$  being the collision frequency. This result can be understood in the framework of the following simplified model. A magnetic surface is characterized by its ripple  $\delta$  given by  $B_{\min}$  and  $B_{\max}$  and defining a boundary in velocity space

$$x_b = \frac{v_{\parallel b}}{v} = \left(1 - \frac{B_{\min}}{B_{\max}}\right)^{1/2} = (2\delta)^{1/2}. \quad (3.3)$$

In simplified mirror theory, the distribution function  $f(x)$  vanishes for  $x_b \leq x \leq 1$ , analogously in stellarators without electric field for  $0 \leq x \leq x_b$ . The stationary solution  $f(x)$  is obtained by solving the eigenvalue problem

$$\frac{d}{dx} \left[ (1-x^2) \frac{df}{dx} \right] = -\alpha f \quad (3.4)$$

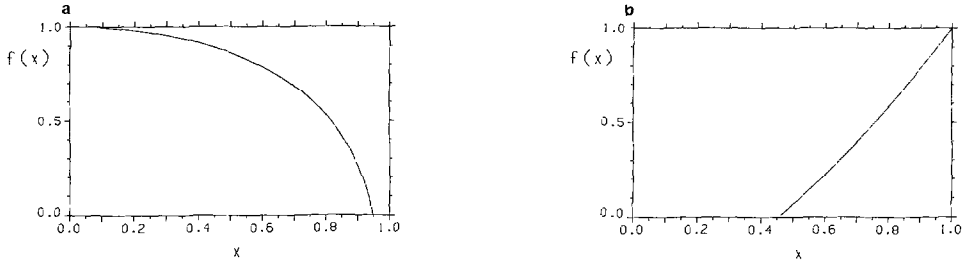


FIG. 4. (a) Typical mirror distribution function  $f(x)$ ,  $x = v_{\parallel}/v$ , in the loss cone regime for  $B_{\max}/B_{\min} = 10$ . (b) Typical stellarator or rippled tokamak distribution function  $f(x)$ ,  $x = v_{\parallel}/v$ , in the loss cone regime for  $\delta = 0.10$ .

for the source strength  $\alpha$  with the boundary conditions  $f(x_b) = 0$  and  $f'(0) = 0$  for the mirror and  $f(1) = 1$  for the stellarator. Figure 4 shows these distribution functions in the mirror case for  $B_{\max}/B_{\min} = 10$  and in the stellarator case for  $\delta = 0.10$ . Figure 5 shows the normalized confinement time  $\tau/\tau_c = 2/\alpha$  in the mirror case as a function of the logarithm of the mirror ratio and in the stellarator case as a function of ripple. In the present context of  $l=2$  stellarators with  $\delta_c \lesssim 0.1$ , the loss rate is given in good approximation by the collision frequency. Figure 6 shows a histogram of a distribution  $f(\psi_0, x) \Delta\psi$ , where  $\psi_0$  was chosen such that  $\delta = 0.1$ .

Comparison of the  $\nu$ , ripple, and plateau regimes yields the following boundaries between these regimes:

$$L_{\nu R}^* \approx 0.78 Q_{\rho} A^{1.2} (l/N)^{0.5}, \quad (3.5)$$

$$L_{RP}^* \approx 2.2 A^{2.35} / lN, \quad (3.6)$$

$$L_{\nu P}^* \approx 0.28 Q_{\rho}^2 l^2, \quad (3.7)$$

as obtained from the asymptotic dependences. Hence, a quite large value of  $Q_{\rho} \gtrsim 2.8 A^{1.2} / l^{1.5} N^{0.5}$  is required for the ripple regime to exist. The actual results, in

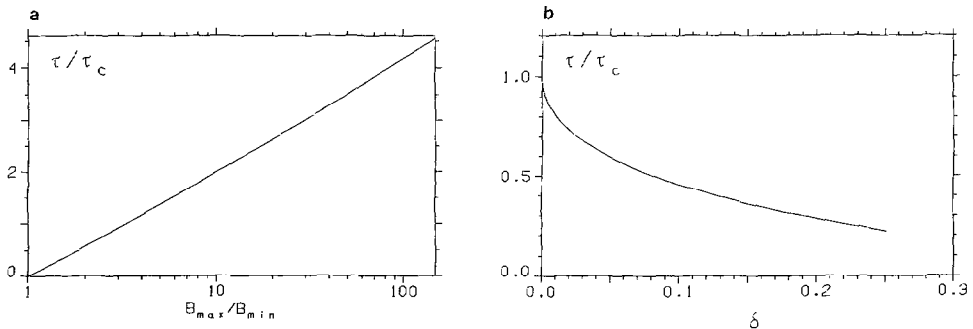


FIG. 5. (a) Mirror confinement times normalized to the collision time versus  $B_{\max}/B_{\min}$ . (b) Stellarator or rippled tokamak confinement times normalized to the collision time versus ripple  $\delta$ .

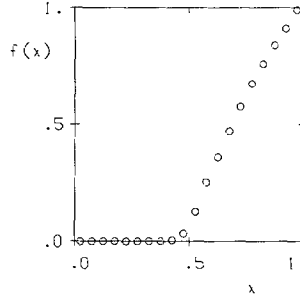


FIG. 6. Stationary distribution function  $f(x)$ ,  $x = v_{||}/v$ , in the  $v$  regime for a rippled tokamak.  $L^* = 10^4$ , 20 collision times,  $Q_\rho = 100$ ,  $R_0/a = 7$ ,  $l = 0.5$ ,  $\delta_c = 0.10$ ,  $\psi = 0.3$ .

which the transitions between the regimes are gradual, show that only for  $Q_\rho > 10^2$  does an increase of the losses due to ripple effects become evident. On the other hand, Eq. (3.5) shows that the maximum loss rate

$$S_{\max}^* \approx 0.36 Q_\rho A^{-1.2} l^{1.5} N^{0.5} \quad (3.8)$$

becomes substantially larger than the plateau loss for sufficiently large  $Q_\rho$ , i.e., for electrons.

#### 4. LOCAL TRANSPORT COEFFICIENTS WITH ELECTRIC FIELD

An important effect of the electric field is its influence on the collisionless orbits of the localized particles [9]. These orbit changes cause the transition from the ripple regime to the so-called  $v$  and  $v^{1/2}$  regimes. The Monte Carlo simulations of the local transport coefficient yield, for  $l=2$  stellarators, the following results in these regimes:

$$D_{1F}^* = 1.0 H^2 v^*, \quad (4.1)$$

$$D_{2F}^* = 0.11 H^{1.5} \sqrt{v^*}, \quad (4.2)$$

$$H = \frac{2}{A} \frac{l}{\rho} \frac{E}{eF}, \quad (4.3)$$

where  $\rho$  is the formal gyro radius,  $E$  the kinetic particle energy, and  $v^* = 1/L^*$ .  $F$  is the electric field on the magnetic surface considered, which has aspect ratio  $A$  and twist  $l$ ;  $F$  is related to the potential  $\phi = \phi_0(1 - \psi)$  by  $F = \phi_0 2r/a^2$ , where  $r$  is the formal radius of the magnetic surface with normalized flux  $\psi$ . Figure 7 shows results for  $Q_\rho = 10^4$ . Equations (4.1) through (4.3) are in accordance with previous analytical results [9] and are valid for  $H > 10$ . In particular, the dependence of the transitions from both the  $v^{-1}$  to  $v^{1/2}$  regimes and the  $v^{1/2}$  to  $v$  regimes is given by

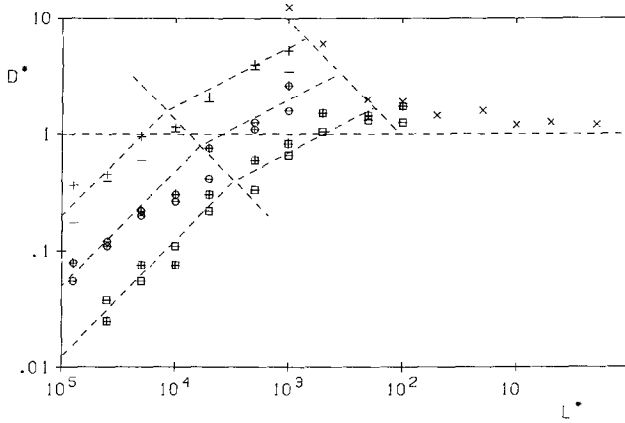


FIG. 7. Normalized transport coefficient  $D^*(L^*)$  in an  $l=2$  stellarator for  $Q_\rho = 10^4$  and various electric fields;  $e\phi_0/E=0$  ( $\times$ ),  $\pm 4$  ( $+$ ,  $-$ ),  $\pm 8$  ( $\circ$ ),  $\pm 16$  ( $\square$ ),  $H=137, 68, 34$ ,  $A=12.5$ ,  $N=5$ ,  $\iota=0.5$ ,  $\delta_e \approx 0.03$ .

$v^* \propto e\phi_0/EQ_\rho$ , so that these transitions occur in the long mean free path regime for electrons. On the other hand, the location of the transitions is proportional to the potential  $\phi_0$ . For example, the transition from the  $v^{-1}$  to the  $v^{1/2}$  regime is given by

$$v^* \approx 3 \frac{A}{\iota} \frac{e\phi_0}{E} \frac{\delta_e}{Q_\rho}. \quad (4.4)$$

If a formal diffusion coefficient is associated with the loss rate found in the  $v$  regime without electric field, Eq. (3.2), it is easy to see that this  $v$  regime is suppressed if  $e\phi_0/E > 1.9 a/R_0$ . Finally, comparison with the transport coefficient in the tokamak banana regime, Eq. (2.4), shows that large potentials in units of the particle energy are needed to approach the neoclassical loss in a tokamak without ripple.

## 5. LOSS RATES WITH ELECTRIC FIELD

With an applied electric field, several basic points have to be observed.

First, the associated poloidal rotation velocity  $v_p$  at the plasma boundary is governed by

$$\frac{v_p}{v} = \frac{e\phi_0}{EQ_\rho}, \quad (5.1)$$

so that for  $e\phi_0/E \approx 1$  the rotation is always slow as compared with thermal velocities, which case is considered here.



Second, the resonant poloidal velocity  $v_{p \text{ res}} = w_{||}/A$ , which destroys the confinement of passing particles, only occurs if

$$\frac{e\phi_0}{E} = \frac{iaQ_\rho}{R}, \quad (5.2)$$

i.e.,  $H = 1$  (Eq. (4.3)) corresponding to quite large potentials in units of the particle energy. Monte Carlo simulations of this case are not considered in the present paper. In particular, the potential is too small for the resonance to occur in the results described in Section 4.

Third, to calculate loss rates according to the scheme described in Section 2, the pitch angle collision operator has to be supplemented by an energy collision operator which keeps the particle kinetic energy an approximate constant. For if the total energy were conserved, the electrostatic confinement properties would dominate the behaviour of the test particle distribution function. Here, the kinetic energy is relaxed with the same time constant which governs the pitch angle scattering:

$$x_{\text{new}} = x_{\text{old}}(1 - \Delta) \pm [(1 - x_{\text{old}}^2) \Delta]^{1/2}, \quad (5.3)$$

$$E_{\text{new}} = E_{\text{old}} + (E - E_{\text{old}}) \Delta, \quad (5.4)$$

where  $\Delta = \Delta t/\tau_{90}$  ( $\Delta t$  time step) and  $x_{\text{new}}$ ,  $x_{\text{old}}$  are the values of the pitch angle and  $E_{\text{new}}$ ,  $E_{\text{old}}$  the values of the kinetic energy,  $E$  being the initial kinetic energy of the test particle. This procedure results in thermodynamic equilibrium of the test particle distribution  $f$  in the applied potential  $\phi$ , i.e.,  $f = f_0 \exp(-e\phi/E)$ , where  $f_0$  is the distribution without applied electric potential. Figure 8 shows stationary

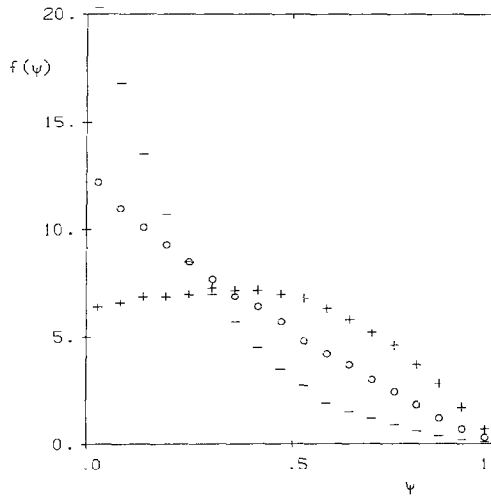


FIG. 8. Stationary distribution functions  $f(\psi)$  with and without electric field in a tokamak in the plateau regime;  $e\phi_0/E = 0$  ( $\circ$ ),  $\pm 2$  ( $+$ ,  $-$ ),  $H = 25$ ,  $L^* = 10$ ,  $Q_\rho = 10^3$ ,  $R_0/a = 10$ ,  $\iota = 0.5$ ,  $10^5$  collision times.

distributions in the tokamak plateau regime which indeed verify this behaviour. Obviously, the condition of quasi-neutrality is not taken into account in the framework of this treatment, so that a cautious interpretation is needed. Since for a given transport coefficient the loss rate is proportional to the gradient at the plasma edge, the loss rate (in contrast to the local transport coefficient) depends on the sign of the electric field: the “attracting” potential ( $e\phi_0 < 0$ ) results in a smaller loss than without electric field, the “repelling” potential ( $e\phi_0 > 0$ ) in a larger one. Figure 9 shows these results for a rather large value of  $Q_\rho = 500$ , where the notion of a local gradient at the boundary applies. Numerically,  $S_+(e\phi_0/E = +2)/S_-(e\phi_0/E = -2) \approx 13$  is found, which is quite close to the theoretical value

$$\frac{S_+}{S_-} = \exp(4) \frac{\int J_0(2.4\sqrt{\psi}) \exp(-2\psi) d\psi}{\int J_0(2.4\sqrt{\psi}) \exp(+2\psi) d\psi}, \quad (5.5)$$

this being 15.6. From Fig. 9 it is also seen that the difference in loss rates becomes less pronounced with increasing mean free path. The ordering relation

$$S_-^* < D_F^* < S_+^* \quad (5.6)$$

remains satisfied. Here  $D_F^*$  is the local transport coefficient with electric field, which, for the case of the axisymmetric tokamak, does not depend on the sign or magnitude of the electric field applied.

Analogous results are found for  $l=2$  stellarators (see Fig. 10), in which all three quantities  $S_-^*$ ,  $D_F^*$ , and  $S_+^*$  are obtained for  $Q_\rho = 500$ . In the lmfp regime the improvement as compared with the loss rate without electric field is of the order  $10^2$ , i.e., the confinement time is  $10^2$  collision times, irrespective of the sign of the potential.

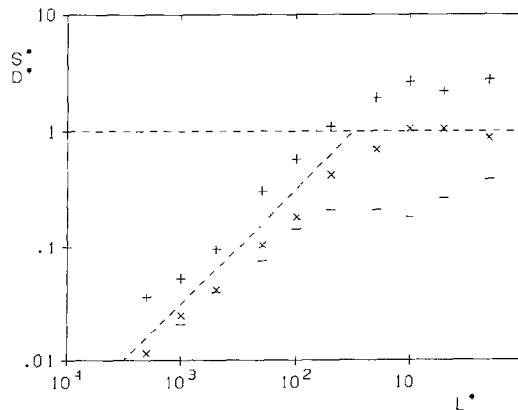


FIG. 9. Normalized loss rates  $S^*$  (+, -) in a tokamak with  $e\phi_0/E = \pm 2$ ,  $Q_\rho = 500$ ,  $R_0/a = 10$ ,  $\iota = 0.5$ . In addition, the normalized transport coefficient  $D^*$  ( $\times$ ) (which is independent of the electric field) is shown;  $Q_\rho = 500$ ,  $A = 10$ ,  $\iota = 0.5$ ,  $H = 21$ . The dashed curve represents the banana regime with  $D_B^* = A^{3/2}/L^*$  (Eq. (2.4)).

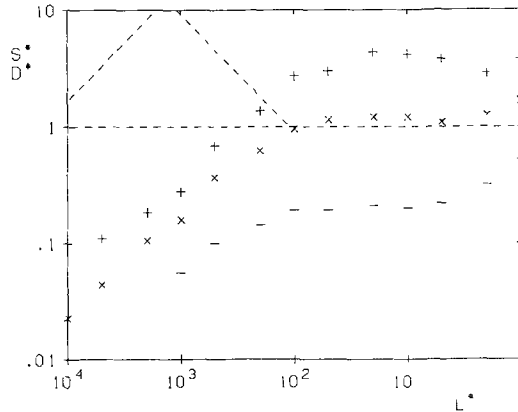


FIG. 10. Normalized loss rates  $S^*$  (+, -) in an  $l=2$  stellarator with  $e\phi_0/E = \pm 2$ ,  $Q_p = 500$ ,  $R_0/a = 8.6$ ,  $N = 5$ ,  $\iota = 0.5$ ,  $\delta_e \approx 0.02$  (at  $A = 17$ ). In addition, the corresponding normalized transport coefficient  $D^*$  ( $\times$ ) (which does not depend on the sign of the electric field) is shown;  $Q_p = 500$ ,  $A = 12.5$ ,  $N = 5$ ,  $\iota = 0.5$ ,  $H = 14$ ,  $\delta_e \approx 0.03$ . The  $\nu^{-1}$  and  $\nu$  regimes are also indicated.

## 6. CONCLUSION

It is shown that Monte Carlo methods can be successfully applied to the computation of neoclassical transport coefficients as well as neoclassical confinement times over wide ranges of mean free paths and ratios of plasma to gyro radius without and with radial electric field. Although the condition of quasi-neutrality has not yet been taken into account, the results obtained in the long mean free path regime suggest that ion confinement is sufficiently improved with an electric potential of the order of the particle energy. Thus, the contribution of electron-electron collisions to neoclassical energy confinement will be of comparable importance; see Eqs. (3.5) and (4.3).

In this paper, only results on tokamaks without and with ripple and  $l=2$  stellarators are presented. Results for advanced stellarators with a more complicated Fourier structure of  $|\mathbf{B}|$  can be obtained without any changes in the computational procedures described. Preliminary results for the W VII AS and the Helias stellarators have already been obtained [7] and will be discussed in future work.

## ACKNOWLEDGMENTS

We are indebted to R. H. Fowler, J. F. Lyon, and J. A. Rome for providing us with their Monte Carlo code.

## REFERENCES

1. A. H. BOOZER AND G. KUO-PETRAVIC, *Phys. Fluids* **24**, 851 (1981).
2. W. LOTZ AND J. NÜHRENBURG, *Z. Naturforsch. A* **37**, 899 (1982); W. DOMMASCHK, W. LOTZ, AND J. NÜHRENBURG, *Nucl. Fusion* **24**, 794 (1984).
3. R. H. FOWLER, J. A. ROME, AND J. F. LYON, *Phys. Fluids* **28**, 338 (1985).
4. H. WOBIG, *Z. Naturforsch. A* **37**, 906 (1982).
5. G. KUO-PETRAVIC, A. H. BOOZER, J. A. ROME, AND R. H. FOWLER, *J. Comput. Phys.* **51**, 261 (1983).
6. *IPP Annual Report 1984* (Max-Planck-Institut für Plasmaphysik, Garching bei München, 1985), p. 119.
7. *IPP Annual Report 1985* (Max-Planck-Institut für Plasmaphysik, Garching bei München, 1986), p. 140.
8. K. MIYAMOTO, *Plasma Physics for Nuclear Fusion* (MIT Press, Cambridge, MA, 1980), p. 198.
9. H. E. MYNICK, *Phys. Fluids* **26**, 2609 (1983).